Evidence for a band broadening across the ferromagnetic transition of $Cr_{1/3}NbSe_2$

W. Z. Hu,[1] G. T. Wang,[1] Rongwei Hu,[2,3] C. Petrovic,[2] E. Morosan,[4] R. J. Cava,[4] Z. Fang,[1] and N. L. Wang[1,*]

[1]*Beijing National Laboratory for Condensed Matter Physics, Institute of Physics, Chinese Academy of Sciences, Beijing 100080, People's Republic of China*

[2]*Condensed Matter Physics and Materials Science Department, Brookhaven National Laboratory, Upton, New York 11973, USA*

[3]*Physics Department, Brown University, Providence, Rhode Island 02912, USA*

[4]*Department of Chemistry, Princeton University, Princeton, New Jersey 08540, USA*

(Received 23 April 2008; revised manuscript received 14 July 2008; published 15 August 2008)

The electronic structure of $Cr_{1/3}NbSe_2$ is studied via optical spectroscopy. We observe two low-energy interband transitions in the paramagnetic phase, which split into four peaks as the compound enters the ferromagnetic state. The band structure calculation indicates the four peaks are interband transitions to the spin up Cr e_g states. We show that the peak splitting below the Curie temperature is *not* due to the exchange splitting of spin-up and spin-down bands, but directly reflects a band broadening effect in Cr-derived states upon the spontaneous ferromagnetic ordering.

DOI: 10.1103/PhysRevB.78.085120 PACS number(s): 78.30.Er, 75.50.Cc, 78.40.Kc

I. INTRODUCTION

Layered transition metal dichalcogenides TX_2 (T=transition metal, X=chalcogen) are among the most studied two-dimensional electronic systems. The charge-density-wave (CDW) instability and its coexistence/competition with superconductivity are central characteristics of this family.[1,2] On the other hand, due to the weak van der Waals interaction between X-T-X sandwich layers, a large variety of atoms and molecules can be intercalated into the interlayer vacant sites, and dramatically change the physical properties.[3–6]

Among various intercalates, the 3d-transition-metal intercalated 2H-type M_xTX_2 are particularly interesting (M=V, Cr, Mn, Fe, Co, Ni; 2H means *two* X-T-X sandwiches in one unit cell, and the compound has a *hexagonal* symmetry). At 1/4 or 1/3 doping, the intercalated 3d ions form an ordered two-dimensional magnetic array and show either ferromagnetic (FM) or antiferromagnetic (AFM) order at low T, depending on the intercalated species and the host compound.[4–6] Transport measurements commonly indicate metallic conductivity in the paramagnetic (PM) state and a more rapid decrease in resistivity in the spin-ordered state. The easy axis of the magnetization can be either parallel or perpendicular to the hexagonal layers for different FM intercalates.[4,5] The types of magnetic ordering encountered provide an interesting venue for exploring spin-related effects, for example, the anomalous Hall effect[7] or the magneto-optical effect, topics of renewed and increased interest due to the recent development of intrinsic mechanism arising from the Berry phase of the Bloch state.[8]

The T-dependent band structure, especially its modification across the FM transition, provides essential information in understanding ferromagnetism. In the itinerant Stoner model,[9] the energy gain in the FM state arises from the exchange interaction, and the collapse of exchange splitting leads to a vanishing magnetic moment above the Curie T. While in the localized model,[10] ferromagnetism originates from the long-range ordered local moments, which are orientation disordered in the PM state. However, practical ferromagnets usually belong to the intermediate regime between the above two extremes, requiring a unified picture which covers the whole range from itinerant to localized ferromagnetism.[11]

In this work, we present an optical spectroscopy study and first-principles calculations on $Cr_{1/3}NbSe_2$ to elucidate the electronic structure change across the FM transition. In comparison with pure 2H-$NbSe_2$, two new interband transitions in the mid- and near-infrared region emerge in $Cr_{1/3}NbSe_2$, which split into four in the FM state. Band structure calculation indicates a strong hybridization between Cr 3d and Nb 4d bands near E_F, and the spin up Cr e_g shows a double-peak character in the density of states (DOS) map. Then the four optical peaks in the FM state are all interband transitions to Cr $e_g(\uparrow)$, and the band broadening in this Cr-derived state is the cause for the peak splitting in the optical response.

II. DETAILS FOR EXPERIMENT AND BAND STRUCTURE CALCULATIONS

Both 2H-$NbSe_2$ and 2H-type $Cr_{1/3}NbSe_2$ single crystals were grown by the vapor transport method. The structure of $Cr_{1/3}NbSe_2$ is shown in Fig. 1. The T-dependent resistivity was obtained by the four-contact technique in a Quantum Design physical properties measurement system (PPMS). The near-normal incident reflectance spectra were measured by a Bruker IFS 66v/s spectrometer in the frequency range from 40 to 25 000 cm^{-1}. An *in situ* gold and aluminum overcoating technique was used to get the reflectivity $R(\omega)$. The real part of conductivity $\sigma_1(\omega)$ is obtained by the Kramers-Kronig transformation of $R(\omega)$.

First-principles calculations based on the local density approximation (LDA) and local spin density approximation (LSDA) were performed to get the electronic structure of $NbSe_2$ and $Cr_{1/3}NbSe_2$, respectively. The calculations were done with our STATE code.[12] We adopt the experimental structure parameters,[13] and an initial Se position z=0.125c for both compounds, then relax the Se ions to their lowest energy positions (z_{Se}=0.132c for 2H-$NbSe_2$; z_{Se}=0.131c for $Cr_{1/3}NbSe_2$). In previous calculation, z_{Se} for 2H-$NbSe_2$ is around 0.118c.[14] The discrepancy arises from different

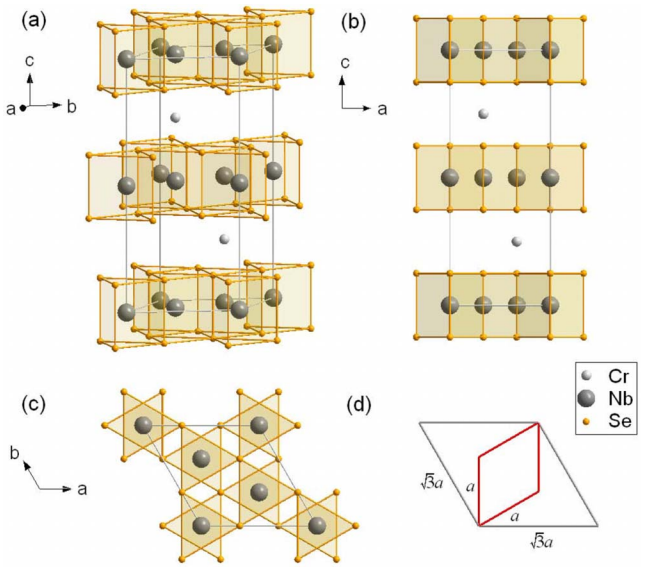

FIG. 1. (Color online) The unit cell of 2*H*-$Cr_{1/3}NbSe_2$: (a) a 3D view; (b) a (010) projection: Cr atoms occupy one third of the octahedral holes in the van der Waals gap; (c) a (001) projection; (d) a comparison of the $NbSe_2$ unit cell (red) and the $Cr_{1/3}NbSe_2$ $\sqrt{3} \times \sqrt{3}$ superlattice (gray).

choices for the atomic coordination. Here we set the Nb position as (0,0,0), not $(0,0,1/4c)$.[14] Note $z_{Se}=0.132c$ in Nb(0,0,0) is in fact equivalent to $z_{Se}=0.118c$ in Nb$(0,0,1/4c)$ coordination.

III. EXPERIMENTAL RESULTS: TRANSPORT AND OPTICAL PROPERTIES

As shown in Fig. 2, a metallic behavior is found for $Cr_{1/3}NbSe_2$ from 300 to 10 K. The resistivity drops more rapidly with decreasing T below 115 K, consistent with the onset temperature of FM ordering.[5,15] Similar transport behavior is observed in other 3*d*-transition-metal intercalates.[4–6] The inset of Fig. 2 focuses on the CDW and superconducting transitions for 2*H*-$NbSe_2$.

The $R(\omega)$ for 2*H*-$NbSe_2$ [Fig. 3(a)] are the same as found in a previous study,[16] except for a new feature in the mid-

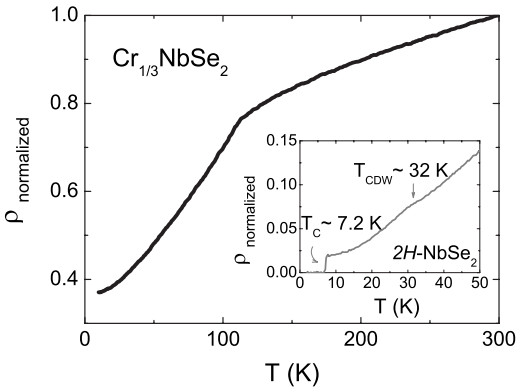

FIG. 2. Normalized T-dependent resistivity for $Cr_{1/3}NbSe_2$. Inset: an expanded plot for the CDW (~32 K) and superconducting transitions (~7.2 K) in 2*H*-$NbSe_2$.

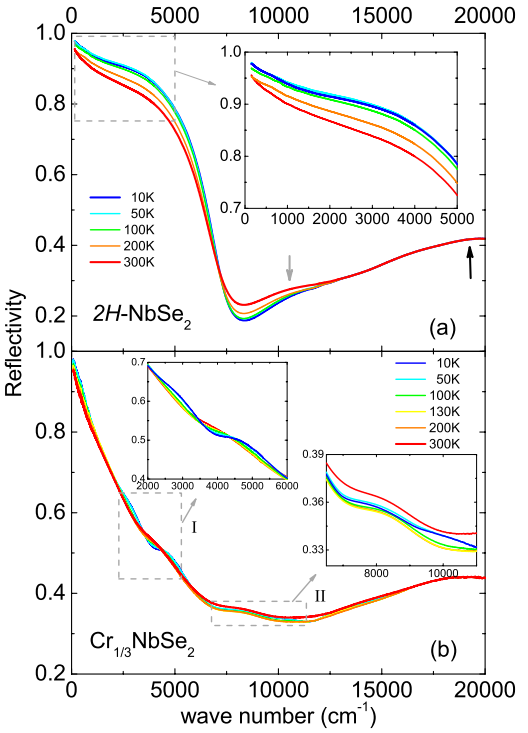

FIG. 3. (Color online) Reflectivity of (a) 2*H*-$NbSe_2$ and (b) $Cr_{1/3}NbSe_2$ below 20000 cm^{-1} at various temperatures. The inset figures amplify the low-frequency characters.

infrared region: $R(\omega)$ at 10 K is suppressed slightly below that at 50 K from 600 to 5000 cm^{-1}. This is intrinsic since the same result was repeatedly obtained, with each study carried out on a fresh, newly cleaved surface. The mid-infrared suppression implies the formation of a partial energy gap on the Fermi surface in the CDW state, which closely resembles that of 2*H*-TaS_2,[17] another CDW-bearing member with a higher T_{CDW} (75 K) and thus a more apparent gap character.

$R(\omega)$ is greatly modified after Cr intercalation [Fig. 3(b)]. The well-defined plasma edge for 2*H*-$NbSe_2$ decays into a overdamped one in $Cr_{1/3}NbSe_2$. Such an overdamped shape might arise from impurity scattering due to Cr disorder, but not the scattering by Cr moments since the shape of the plasma edge is almost unchanged from FM to PM states. The most interesting features are two additional peaks around 4300 and 8500 cm^{-1} at 300 K, and their splitting below 115 K. No similar feature is found in the host compound.

The low-energy interband transitions in $Cr_{1/3}NbSe_2$ can be more clearly resolved in the real part of the conductivity $\sigma_1(\omega)$, as illustrated in Fig. 4(a). Beside the Drude component, two peaks around 4300 and 8500 cm^{-1} at 300 K split into four peaks near 2600, 4700, 8400, and 10500 cm^{-1} in the FM state. In order to extract these features from the background, we fit $\sigma_1(\omega)$ by the Drude-Lorentz model.[18] In the inset of Fig. 4(a), the fitting curves of 10 and 300 K match the original data well. Subtracting the Drude components and the high-energy interband transitions from $\sigma_1(\omega)$, we then get a clear picture of the absorption peaks and their splitting in Fig. 4(b): the peak δ_1 (4250 cm^{-1}) at 300 K splits into α_1 (2610 cm^{-1}) and β_1 (4690 cm^{-1}) at 10 K;

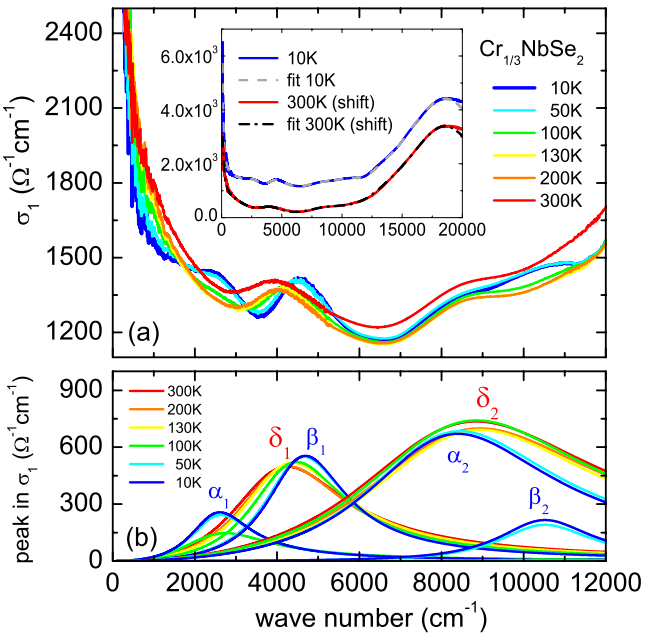

FIG. 4. (Color online) (a) $\sigma_1(\omega)$ for $Cr_{1/3}NbSe_2$ below 12 000 cm^{-1}. The inset illustrates the experimental data and the Drude-Lorentz fitting for 10 and 300 K below 20 000 cm^{-1}. The raw data and the fitting for 300 K are shifted down by 1000 Ω^{-1} cm^{-1} for clarity. (b) The first four Lorentz terms extracted from the fitting.

the peak δ_2 (8840 cm^{-1}) splits into α_2 (8400 cm^{-1}) and β_2 (10 520 cm^{-1}). The splitting energies $\beta_1-\alpha_1$ and $\beta_2-\alpha_2$ are almost the same, hence those peaks should have a similar origin. The apparent spectral difference for $NbSe_2$ and $Cr_{1/3}NbSe_2$ indicates Cr intercalation is not a simple charge transfer process. Detailed information about the band structure is required.

We note that the spectral difference (i.e., the splitting of the interband transitions) at 100 and 130 K in the near-infrared region is obscure. This is understandable as those features in $R(\omega)$ are close to the reflectivity minimum and the overall peak strengths are rather weak. In addition, both $T=100$ K and 130 K are very close to the FM transition temperature (115 K), therefore fluctuation effect is also prone to influence the spectra near the critical temperature. On the other hand, in our overcoating technique for reflectance measurement, the sample is not in exchange gas but in vacuum (better than 3×10^{-7} torr); the measurement becomes relatively surface sensitive in such high energy. A more detailed inspection of temperature variations in $\sigma_1(\omega)$ for the FM phase, which requires keeping the sample at low temperature for a long time, becomes impractical. However, the splitting indeed turns more apparent as the temperature goes down to 50 and 10 K from our current data, which confirms the connection between the splitting in the optical conductivity and the FM ordering.

IV. THEORETICAL RESULTS: THE GROUND-STATE BAND STRUCTURE

Conventionally, the band-structure modification after intercalation is understood by the rigid-band model: the host band structure is unchanged upon intercalation, meanwhile, electrons from the guest species fill the host conduction band, thus raise the chemical potential. However, our optical data apparently violate the rigid-band model for the emergence of new interband transitions in Cr-doped $NbSe_2$ and their further splitting at low T. To understand these low-energy interband transitions, details about the band structure for both the pure and the Cr-intercalated compounds are required.

We obtain the ground-state electronic structure for $NbSe_2$ and $Cr_{1/3}NbSe_2$ by first-principles calculations. The projected density of states (PDOS) for $2H$-$NbSe_2$ is shown in Figs. 5(a) and 5(b). The crystal structure of $2H$-$NbSe_2$ is the same with that of $Cr_{1/3}NbSe_2$ if Cr atoms were removed. Each Nb

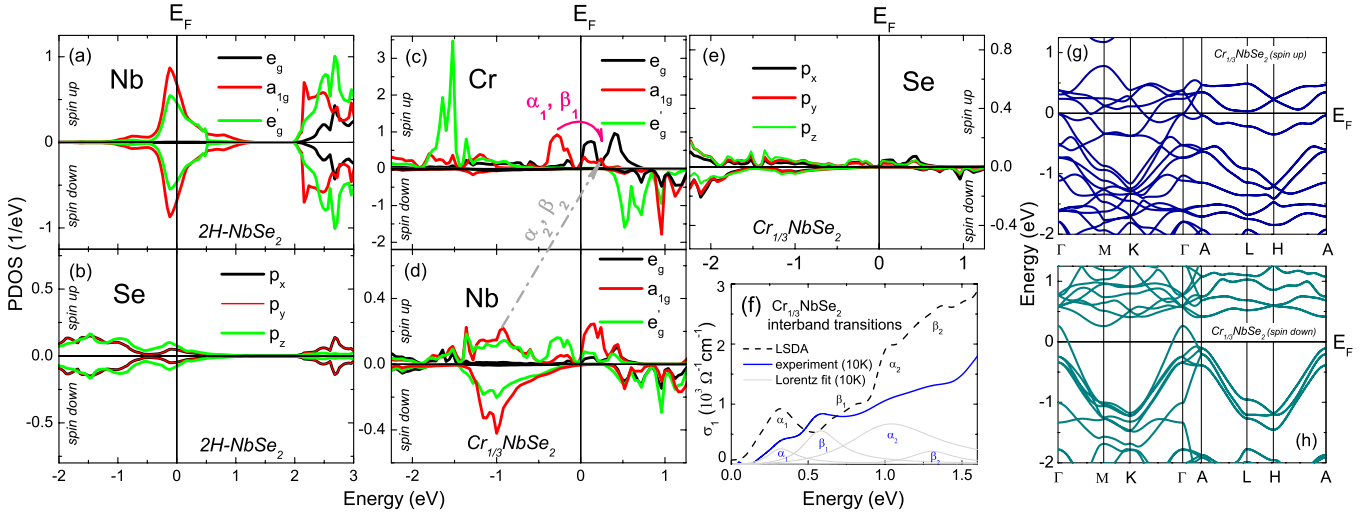

FIG. 5. (Color online) The PDOS for $2H$-$NbSe_2$: (a) Nb, and (b) Se. The PDOS for ferromagnetic $Cr_{1/3}NbSe_2$: (c) Cr, (d) Nb (Ref. 20), and (e) Se. (f) Calculated interband transitions for $Cr_{1/3}NbSe_2$ in the FM ground state (black dash line), comparing with the experimental data at 10 K (the Drude term is subtracted) (blue solid line), and the Lorentz fit in Fig. 4(b) (light gray solid line). The band structure for ferromagnetic $Cr_{1/3}NbSe_2$: (g) the spin-up and (h) the spin-down band.

is in trigonal prismatic coordination with six Se neighbors so the Nb 4*d* states are split into: a_{1g} (d_{z^2}) state, e_g' doublet (d_{xy};$d_{x^2-y^2}$), and e_g doublet (d_{yz};d_{zx}). Far below the Fermi energy, the total density of states is of Se 4*p* character. The tail of this Se band hybridizes with Nb (a_{1g},e_g') complex and extends above E_F. A high density of states at the Fermi energy consists with the optical observation of a well-defined plasma edge in 2*H*-$NbSe_2$.

We note that the partially filled Nb conduction band is frequently referred to as "d_{z^2}" band in the early studies. However, recent calculations on 2*H*-$NbSe_2$ (Ref. 14) show that the half-filled conduction band has d_{z^2} symmetry around the Γ point of the Brillouin zone, and ($d_{x^2-y^2}$, d_{xy}) symmetry around the *K* point. Similar result is reproduced in Fig. 5(a) that both a_{1g} (d_{z^2}) and e_g' ($d_{x^2-y^2}$, d_{xy}) contribute to the PDOS of the half-filled conduction band.

Figure 5(c)–5(e) shows the PDOS for $Cr_{1/3}NbSe_2$ in the FM ground state. Since Cr is in a trigonally distorted $CrSe_6$ octahedron,[5] the Cr 3*d* bands are split into t_{2g} (which is further split into a_{1g} and e_g') and e_g states. In the spin-up channel, the Cr e_g' state is localized and fully occupied, while the Cr a_{1g} state and e_g doublet have weak itinerant character, and strongly hybridize with Nb conduction band in the range −0.5–0.5 eV across E_F. All the spin-down Cr 3*d* bands are unoccupied. From Fig. 5(g) and 5(h), one will find that $Cr_{1/3}NbSe_2$ is metallic with a Fermi level crossing in both spin directions.

Comparing with 2*H*-$NbSe_2$, the half-filled Nb conduction band is now almost filled up in $Cr_{1/3}NbSe_2$, with a large removal of DOS at the Fermi energy, leading to a marked reduction in the free carrier spectral weight. Although there is a strong hybridization between Cr t_{2g} (↑) and e_g' (↑) states near E_F, the occupied Nb states in the spin-down projection is almost unaffected after intercalation, besides a shift of the chemical potential.

V. DISCUSSIONS

A. Origin of the low energy interband transitions

In comparison with the band-structure calculations, we can identify the origin of the experimental interband transitions (associated with the joint density of states) at low *T*.

For $NbSe_2$, the close-to-E_F interband transition from occupied Se to unoccupied Nb states is the origin of the first peak around 12 000 cm^{-1} in Fig. 3(a). While the second peak at 20 000 cm^{-1} is the Nb *d* to *d* hopping from E_F to the lowest empty state. Such *d*-*d* transition is not forbidden with the help of Se 4*p* hybridization.

For $Cr_{1/3}NbSe_2$, all possible low-energy (<1.5 eV) interband transitions in the FM ground state include Cr-to-Cr, Nb-to-Nb, and Cr-to-Nb (also Nb-to-Cr) transitions. Note the PDOS scales for Figs. 5(c)–5(e) are different that Cr has apparently larger density of states than that of Nb or Se, so Cr-Cr and Cr-Nb transitions should dominate the low-energy interband optical peaks. As shown in Fig. 5(g), Cr e_g(↑) bands have rather special dispersion: they are flat near the band bottom and top but dispersive elsewhere (which can be better resolved along A-L-H-A), so it has a double-peak PDOS. Then the two peaks, α_1 and β_1, in $\sigma_1(\omega)$ mainly come from the spin-up Cr $a_{1g} \rightarrow$ Cr e_g transition, and the α_2 (1.04 eV) and β_2 (1.30 eV) peaks are mainly contributed by the occupied spin up Nb (a_{1g},e_g') → Cr e_g transition. Other Cr-Cr or Cr-Nb transitions exceed the energy scope in Fig. 4(b), while the low-energy Se-Nb transition in $NbSe_2$ shifts to higher energies because Cr intercalation raises the chemical potential.

The predicted interband contributions in $\sigma_1(\omega)$ from the LSDA calculation are shown in Fig. 5(f). The experimental data with the removal of the Drude component are also presented for comparison. In general, the theoretical result qualitatively reproduces the experimental observation of a four-peak character in the low-energy optical response.

B. Splitting of the optical peaks

Since the Curie-Weiss PM state is a spin-disorder system that the orientation and amplitude of neighboring spins would fluctuate with temperature, one cannot calculate the PM band from first principles. However, the band modification across the FM transition can be speculated from the changes in optical interband transitions.

As Cr e_g(↑) is the common final state for the four interband transitions in the FM ground state, then the two-to-four splitting of the optical peaks should be caused by a splitting, or more generally, a band broadening, in this common e_g state. Provided Cr e_g(↑) turns narrower in the PM state, the interband transitions α_i and β_i are indistinguishable. The band width for a correlated electronic system is related to the hopping integral between neighboring sites, then the long-range ordering of Cr local moment favors a broader bandwidth from PM to FM state. The spin-up Cr a_{1g} and e_g have partial itinerant character with a PDOS "tail" at E_F [Fig. 5(c)]. Therefore the lowering (i.e., gain) of the kinetic energy of carriers in the FM transition would lead to the conduction-band broadening.[19] Here the phase transition does not apparently change the Drude response in $Cr_{1/3}NbSe_2$, indicating the conducting carriers are mainly of Nb 4*d* character, thus are less affected by possible effective mass reduction when the Cr-derived bands turn broader in the FM phase.

As shown above, the interband peak splitting is a band broadening effect in Cr e_g doublet; now further discussions on other possibilities are necessary.

One possible cause for the band modification is a structure distortion, which splits the degenerated e_g into two separated states. Here we should emphasize that the relaxed Se position in our calculation indicates a trigonal distorted $CrSe_6$ octahedra (along the c axis) in the FM ground state, but it apparently does not change the degeneracy of the e_g doublet (d_{zx};d_{yz}). In fact, the double-peak PDOS for Cr e_g(↑) is not two separated states, but due to special band dispersion, so the splitting of the optical peaks is not caused by possible structural distortion.

Another possible case is the exchange splitting. Regardless of the detailed band structure for this specific material, the splitting in the interband transition for a ferromagnet is generally attributed to the exchange splitting: when magnetism is on the itinerant side, the PM phase will have some set

of absorption peaks, and in the FM phase each of them will split into two, reflecting the fact that the exchange splitting is not rigid. However, our band-structure calculations rule out such a possibility. As shown in Fig. 5(c), although the spin-up Cr a_{1g} and e_g have a weak itinerant character, the Cr $3d$ bands are mainly localized; therefore the dominating magnetic mechanism for $Cr_{1/3}NbSe_2$ is away from the itinerant side. In the Curie-Weiss PM state, the Cr $3d$ local moments do not vanish. Then the only close-to-E_F band, which might experience spin polarization from the PM to FM state, is the Nb $4d$ conduction band [Fig. 5(d)]. However, one cannot find any Nb-related interband transitions which satisfy: (1) a 0.5–0.7 eV and 1–1.2 eV gap for both spin projections and (2) a 0.25 eV energy difference for the common hopping in different spin channels (as a 2000 cm^{-1} splitting from optical measurements). In fact, the magnetic moment for Nb atom is less than $0.03\mu_B$ (while Cr moment is $2.6\mu_B$) from our calculation; hence the Nb spin polarization is so weak that it can be neglected, so the splitting of the interband transitions is irrelevant to the exchange splitting.

Here some complementary discussion on the PM band structure should also be added. In the Curie-Weiss paramagnetic state, there is no spin polarization for the energy band, and the optical response from different spin channels have equal contribution to $\sigma_1(\omega)$. As shown above, we conclude that the "spin up" Cr e_g turns narrower in the PM state. Here the spin label was used to better describe this specific band when comparing to the FM case. One should keep in mind that the two spin channels are mixed in the PM state, reflecting the fluctuation of the local spins. However, such a band mixing will not bring new low-energy interband transitions. Note α_i and β_i (i=1,2) all come from Cr-related bands, which are mainly localized and has a large splitting in different spin projections in the FM ground state [Fig. 5(c)]; furthermore, possible spin polarization in the FM state for the Nb- and Se-related bands are rather weak, and the band mixing in the PM state will not bring new peaks for the low frequency $\sigma_1(\omega)$.

Finally, it should be noted that the qualitative electronic structure around Fermi level for $Cr_{1/3}NbSe_2$ is not sensitive to the on-site Coulomb repulsion U of Cr site due to the strong Cr-Nb hybridization. We have tried a LSDA+U (U =3.0 eV for Cr site) calculation; the low-energy optical conductivity is not qualitatively changed (except the α_1 and β_1 peaks are weaker compared to LSDA).

VI. CONCLUSION

We report a combined optical spectroscopy study and first-principles calculations on $2H$-type $NbSe_2$ and the ferromagnetic intercalated compound $Cr_{1/3}NbSe_2$. A weak mid-infrared suppression in $R(\omega)$ of $2H$-$NbSe_2$ testifies the existence of a CDW-induced partial gap on the Fermi surface. For $Cr_{1/3}NbSe_2$, the appearance of new interband transitions and their remarkable T evolution are direct experimental evidence for the invalidity of the rigid-band model. The multipeak feature in $\sigma_1(\omega)$ has been clearly extracted by a Drude-Lorentz fitting. Based on the LSDA calculation, we found that the four optical peaks in the FM phase are interband transitions involving both the intercalated Cr $3d$ and the host Nb $4d$ states. Considering the temperature evolution for these optical interband transitions, we further conclude that their splitting from PM to FM phase is not an exchange splitting effect, but a dispersion modification (broadening) in the spin up Cr e_g doublet, which have partial itinerant character and strongly hybridize with Nb $4d$ states. Such an evident band broadening in a rather close-to-E_F $3d$ state requires further experimental investigations, which might provide new insight into understanding the ferromagnetism induced band modification across the phase transition.

ACKNOWLEDGMENTS

This work is supported by the National Science Foundation of China, the Knowledge Innovation Project of the Chinese Academy of Sciences, and the 973 project of the Ministry of Science and Technology of China. The work at Brookhaven National Laboratory is operated for the U.S. Department of Energy by Brookhaven Science Associates (Grant No. DE-Ac02-98CH10886), and at Princeton by the National Science Foundation of the USA.

*nlwang@aphy.iphy.ac.cn

[1] E. Morosan, H. W. Zandbergen, B. S. Dennis, J. W. G. Bos, Y. Onose, T. Klimczuk, A. P. Ramirez, N. P. Ong, and R. J. Cava, Nat. Phys. **2**, 544 (2006).

[2] L. Fang, Y. Wang, P. Y. Zou, L. Tang, Z. Xu, H. Chen, C. Dong, L. Shan, and H. H. Wen, Phys. Rev. B **72**, 014534 (2005), and references therein.

[3] S. J. Hillenius and R. V. Coleman, Phys. Rev. B **20**, 4569 (1979); J. F. Garvin, Jr. and R. C. Morris, *ibid.* **21**, 2905 (1980).

[4] R. H. Friend, A. R. Beal, and A. D. Yoffe, Philos. Mag. **35**, 1269 (1977).

[5] S. S. P. Parkin and R. H. Friend, Philos. Mag. B **41**, 65 (1980); **41**, 95 (1980).

[6] E. Morosan, H. W. Zandbergen, Lu Li, Minhyea Lee, J. G. Checkelsky, M. Heinrich, T. Siegrist, N. P. Ong, and R. J. Cava, Phys. Rev. B **75**, 104401 (2007).

[7] J. G. Checkelsky, Minhyea Lee, E. Morosan, R. J. Cava, and N. P. Ong, Phys. Rev. B **77**, 014433 (2008).

[8] Y. Yao, Y. Liang, D. Xiao, Q. Niu, S. Q. Shen, X. Dai, and Z. Fang, Phys. Rev. B **75**, 020401(R) (2007).

[9] E. P. Wohlfarth, Rev. Mod. Phys. **25**, 211 (1953).

[10] P. W. Anderson, *Solid States Physics* (Academic, New York, 1963), Vol. 14, p. 99.

[11] T. Moriya, in *Metallic Magnetism*, edited by H. Capellmann (Springer, Berlin, 1987).

[12] Zhong Fang and Kiyoyuki Terakura, J. Phys.: Condens. Matter **14**, 3001 (2002).

[13] J. M. Voorhoeve, Nee Van Den Berg, and M. Robbins, J. Solid

State Chem. **1**, 134 (1970).
[14] M. D. Johannes, I. I. Mazin, and C. A. Howells, Phys. Rev. B **73**, 205102 (2006), and references therein.
[15] F. Hulliger and E. Pobitschka, J. Solid State Chem. **1**, 117 (1970).
[16] S. V. Dordevic, D. N. Basov, R. C. Dynes, and E. Bucher, Phys. Rev. B **64**, 161103(R) (2001).
[17] W. Z. Hu, G. Li, J. Yan, H. H. Wen, G. Wu, X. H. Chen, and N. L. Wang, Phys. Rev. B **76**, 045103 (2007).
[18] M. Dressel and G. Grüner, *Electrodynamics of Solids* (Cambridge University Press, Cambridge, England, 2002).
[19] J. E. Hirsch, Phys. Rev. B **59**, 436 (1999).
[20] There are two types of Nb sites (Fig. 1): Nb1 has no direct Cr neighbor along the *c* axis, while Nb2 has one. Besides a weaker hybridization with Cr 3*d* states, the Nb2 PDOS shows no intrinsic difference with that of Nb1, so we only plot the Nb1 case in Fig. 5(d). Note the Nb2 to Cr hopping does not contribute to the in-plane $\sigma_1(\omega)$.